XVIII International Conference on Water Resources
CMWR 2010
J. Carrera (Ed)
CIMNE, Barcelona 2010

DOWNSCALING: FINE-SCALE CONDUCTIVITY IDENTIFICATION BY INVERSE MODELLING

Anna Trykozko

ICM, University of Warsaw
Pawinskiego 5a, 02-106 Warszawa, Poland
e-mail: a.trykozko@icm.edu.pl, web page: http://www.icm.edu.pl

Key words: inverse problem, conductivity, double constraint method

Summary. Determination of conductivities from measured or computed head-flow rate pairs is done by inverse modelling. Downscaling, in turn, is inverse modelling applied to determine fine-scale conductivities in coarse-scale grid blocks, in such a way that the boundary conditions arising from a coarse-scale model are honoured at the fine-scale. This way downscaling may be considered as a practical complement to upscaling, if conductivities at a coarse-scale level are obtained by upscaling or, in particular, by homogenization.

We apply the Double Constraint method. This iterative method is based on the Electrical Impedance Tomography approach. The method is discussed and exemplified. Computational examples present applications to far-field downscaling. Finite elements are used as a discretization method.

1 INTRODUCTION

Inverse modelling applied to hydrogeological problems mostly deals with the determination of hydraulic conductivities based on measured or computed heads and flow rates[1, 2]. From the mathematical point of view, the problem of identification of the internal properties of an object from boundary measurements belongs to the class of ill-posed problems, which results in the need of regularization approaches[3, 4] and in the development of other frameworks to handle the problem[5, 6].

The Double Constraint method is a relatively simple approach based on the Electrical Impedance Tomography concept[7]. Its main advantages are robustness and easy implementation, enabling to base computations on any standard flow code with some post-processing added. We apply this approach to the downscaling problem.

By downscaling we mean a special case of inverse modelling applied to determine fine-scale conductivities in coarse-scale grid blocks in such a way that the boundary conditions arising from a coarse-scale model are honoured at the fine scale. This work is a continuation of ideas presented in[1, 8], and at the same time may be viewed as a complement to[9]. Instead of regular heterogeneity patterns used in[8], we base our computational experiments on randomly generated initial conductivity patterns. As opposed to applications aiming at detecting the shape of a body based on different conductivity properties[5,7,10], our main interest is to determine a global heterogeneous field ensuring consistency of boundary conditions rather

than determining precisely the shape of an object.

2 DOWNSCALING AS AN INVERSION PROBLEM

Downscaling, if defined as an inverse to upscaling, may be viewed as a problem of substituting a homogeneous block with a fine-scale heterogeneous conductivity distribution in such a way that the boundary conditions coming from the coarse scale are satisfied. The fine-scale conductivity may originate from our knowledge before upscaling, or may come from any assumptions about the heterogeneity pattern distribution[8], or may be a randomly generated field meeting some statistical criteria.

Two types of boundary conditions, both flux and piezometric head, are specified simultaneously on the block edges, what over specifies the problem in a way that either flux boundary conditions are satisfied, but heads boundary conditions are violated, or head boundary conditions are satisfied, but flux boundary conditions are violated. As a solution of the above contradiction we propose to modify the initial fine-scale conductivity field in such a way that both flux and head boundary conditions are satisfied. This way we come up with the following reconstruction problem: based on boundary data, find an approximation of the conductivity distribution in the interior of a domain Ω. For simplicity reasons only the 2D case will be considered.

All considerations are based on the equation for incompressible and undeformable flow

$$-\nabla \cdot k(x,y)\nabla\varphi = 0\,, \tag{1}$$

$k(x,y)$ - space-varying fine-scale conductivity, φ - piezometric head. Equation (1) may be equivalently written in a form of a continuity equation and Darcy's law:

$$\begin{aligned} \nabla \cdot \mathbf{q} &= 0\,, \\ \mathbf{q} &= -k(x,y)\,\nabla\varphi\,. \end{aligned} \tag{2}$$

Boundary conditions of two types are considered on $\partial\Omega$: Dirichlet boundary conditions $\varphi|_{\partial\Omega} = \Phi$, Φ given function, or Neumann boundary conditions $-k\dfrac{\partial\phi}{\partial n}\Big|_{\partial\Omega} = \Psi$, Ψ given function.

The presented approach is strictly linked to a numerical method applied in order to solve (1). All the computations are performed with the finite element method using linear basis functions defined over triangular meshes.

2.1 Double Constraint Method

The Double Constraint Method (DC) may be viewed as a direct successor of the Electrical Impedance Method[1, 7]. Assume that initial fine-scale conductivity pattern $k(x,y)$ is given in Ω together with two independent sets of boundary conditions which are fluxes (Neumann-type boundary condition) and heads (Dirichlet-type boundary condition) defined on $\partial\Omega$. The DC method is an iterative method; in every step equation (1) is solved twice. In a forward run, denoted as *run_F*, it is solved with Neumann boundary conditions, with fluxes having

components $q_x^F = -k\,\partial\varphi^F/\partial x$ and $q_y^F = -k\,\partial\varphi^F/\partial y$ obtained as a solution. In the second forward run, denoted as *run_H*, Dirichlet boundary conditions are imposed and values of the components $h_x^H = \partial\varphi^H/\partial x$ and $h_y^H = \partial\varphi^H/\partial y$ of the head gradients are computed.

Taking into account fluxes $\mathbf{q}^F = (q_x^F, q_y^F)$ and head gradients $\nabla\varphi^H = (h_x^H, h_y^H)$, the residual $R = \mathbf{q}^F + k\nabla\varphi^H$ may be seen as a measure of the discrepancy between the solutions of *run_F* and *run_H*. Therefore, the aim is to minimize

$$R = \int_\Omega \left(\mathbf{q}^F + k\nabla\varphi^H\right)\cdot\left(\mathbf{q} + k\nabla\varphi^H\right)d\Omega\,. \tag{3}$$

Here come the links to the numerical method used in order to solve (1). We apply linear elements, therefore the finite element formulation yields fluxes and gradients defined element-wise, which are moreover constant within elements. As a consequence, the integral over Ω can be replaced with a summation of integrals over the elements (triangles) Ω_i.

$$R = \sum_i \int_{\Omega_i} \left(\mathbf{q}^F + k\nabla\varphi^H\right)\cdot\left(\mathbf{q}^F + k\nabla\varphi^H\right)d\Omega_i\,.$$

Conductivities k_i are assumed constant in each element. Minimization of *R* by modifying k_i requires $\partial R/\partial k_i = 2\int_{\Omega_i}\left(\mathbf{q}^F\cdot\nabla\varphi^H + k_i\,\nabla\varphi^H\cdot\nabla\varphi^H\right)d\Omega_i = 0$ for all elements Ω_i. Since fluxes and gradients are constant within elements we have $\partial R/\partial k_i = 2\left(\mathbf{q}^F\cdot\nabla\varphi^H + k_i\nabla\varphi^H\cdot\nabla\varphi^H\right)A_i = 0$, A_i - element area. This results in the formula for the updated conductivity in each triangle, $k_i = -\mathbf{q}^F\cdot\nabla\varphi^H/\left(\nabla\varphi^H\cdot\nabla\varphi^H\right)$, which can also be written as the "update equation"

$$k_i^{m+1} = k_i^m\,(\nabla\varphi^F\cdot\nabla\varphi^H)/(\nabla\varphi^H\cdot\nabla\varphi^H)\,. \tag{4}$$

Iterations should result in modifications of the "old" conductivity $k^m(x,y)$ to a "new" conductivity $k^{m+1}(x,y)$ such that $k^{m+1}\to k^m$ and the solutions of *run_F* and *run_H* come sufficiently close to each other.

2.2 Example in 1D

A 1D example is simple yet very instructive. Consider an interval consisting of *n* subintervals of lengths d_1, d_2, ..., d_n. Two sets of boundary conditions are given: heads φ_1 and φ_n, and fluxes q_1 and q_n. Because of continuity we have $q_1 = q_n = q$ all over the domain. Any arbitrary initial conductivity values, k_1^0, k_2^0, ..., k_n^0 are assigned to the appropriate subintervals; see Fig. 1.

The solution of *run_F* of the DC method is immediate and yields fluxes $q^F = q$ in all

subsections. The solution of *run_H* yields head gradients in subsections equal to $\nabla\varphi_i^H = ((\varphi_n - \varphi_1)/k_i^0)/(\sum_{i=1}^{n}(1/k_i^0)\cdot d_i) = q^H/k_i^0$. Therefore, the updated conductivities in the subsections are equal to $k_i^1 = k_i^0 \nabla\varphi_i^F / \nabla\varphi_i^H = k_i^0 q^F / q^H$. As a consequence, the ratio between the conductivities in any two subsections is preserved. In the 1D case the solution is obtained in one iteration. In the sense of honouring all the equations it is also true in 2D and 3D.

Figure 1: Example in 1D

2.3 2D problem: anisotropy

Extending the considerations presented in Section 2.2, rather than using the equation (4) for computing new conductivities, we can apply the formulae

$$k_x^{m+1} = k_x^m h_x^F / h_x^H, \quad k_y^{m+1} = k_y^m h_y^F / h_y^H. \tag{5}$$

As a consequence, even if the initial conductivities are scalar quantities, the modified conductivities may exhibit artificial anisotropy, which may be considered as a disadvantage. Artificial anisotropy may easily be eliminated by using (4) or by a "mixture rule", for instance $k^m = (k_x^m)^{\beta_x} (k_y^m)^{\beta_y}$ with $\beta_x + \beta_y = 1$. (If $\beta_x = \beta_y = 1/2$ this is referred to as square root isotropization.[1, 8]) Even if one of these isotropic formulas are used, controlling the 'amount' of anisotropy arising in consecutive iterations may prove useful as a termination criterion for iterations. The more the modified conductivity field is consistent with the two sets of boundary conditions, the less anisotropy appears in (5).

It is possible to derive a variant of the DC method capable to obtain a fine-scale conductivity with given anisotropy ratio $k_x/k_y = \alpha$ (for $\alpha = 1$ the medium is isotropic). Extension of (4) is straightforward yielding $k_y^{m+1} = k_y^m (\tilde{\nabla}\varphi^F \cdot \tilde{\nabla}\varphi^H)/(\tilde{\nabla}\varphi^H \cdot \tilde{\nabla}\varphi^H)$ with $\tilde{\nabla}\varphi = (\alpha\partial\varphi/\partial x, \partial\varphi/\partial y)$. Like (4), also (5) gives a good starting point to obtain a fine-scale conductivity with given anisotropy ratio α. Modified conductivities in elements with the specified anisotropy ratio are computed using the following mixture rule: $k_y^{m+1} = (k_x^m/\alpha)^{\beta_x} (k_y^m)^{\beta_y}$, $k_x^{m+1} = \alpha k_y^{m+1}$, where k_x^m and k_y^m come from (5). Anisotropy aspects will be the subject of our studies in the future.

3 NUMERICAL EXPERIMENTS

Computational examples were performed in 2D domains, meshed with triangles. The mesh consisted of 421 nodes and 800 elements. As an initial approximation of the fine-scale conductivity we used random conductivity fields, generated with the Matlab code[11]. We

present results obtained for three fields, generated for the 2D exponential model[11] with different values of variance; see Fig. 2. In all three cases the mean-log conductivity was set equal to 1. Parameters of the test fields are summarized in Table 1. Thus obtained fine-scale conductivities were mapped onto the computational mesh.

Parameter	Case 1	Case 2	Case 3
variance	0,5	1	2
correlation length in x and y	5	5	3
minimal value of conductivity	3,0440E-1	5,7548E-2	8,4033E-3
maximal value of conductivity	4,5435E+2	1,0712E+3	5,6651E+4

Table 1: Summary of parameters used in computations

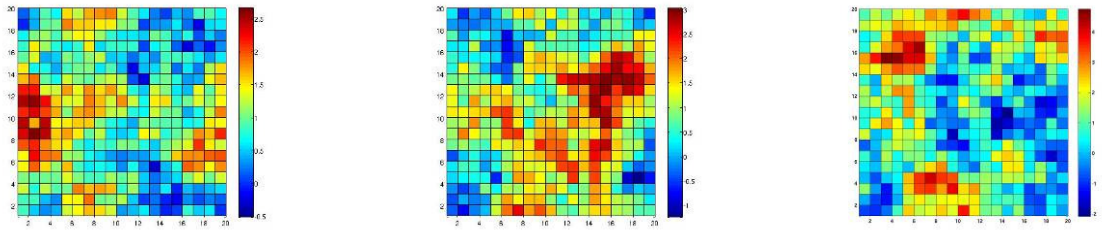

Case 1 Case 2 Case 3

Figure 2: Initial log-conductivity distribution

3.1 Boundary conditions

When applying downscaling, the boundary conditions are to be defined in an accordingly adjusted way. As compared to standard inverse problems, information coming from the boundary is less precise than in the case of direct measurements.

At downscaling we consider one homogeneous grid block together with two sets of boundary conditions simultaneously defined, both of the Dirichlet and Neumann types. The boundary conditions originate from the solution computed by the coarse-scale model. As a consequence, all we have are the values of heads in the corners of the grid block and the values of fluxes through its edges. Specified in this way our boundary conditions do not reflect the heterogeneity we are going to reconstruct.

In our procedure we 'fill' the so far homogeneous block with a heterogeneous, in our case randomly generated, conductivity pattern. In order to make the boundary conditions consistent with conductivities assumed at the fine scale, we modify the original coarse-scale boundary conditions and replace them with fine-scale boundary conditions.

The fine-scale boundary conditions are such that the total inflow through all boundary (fine-scale) cells is equal to the inflow calculated by the coarse-scale model. If Q denotes the total flux through the block's edge, then a flux Q_i related to a centre of a small-scale boundary edge is equal to $Q_i = Q k_i d_i / \sum_i k_i d_i$. In a similar way, the average of heads on boundary (fine-scale) cells is equal to the average head calculated by the coarse-scale model.

The total difference in heads $\Delta\varphi$ along a boundary edge of the block is distributed among fine-scale edges in the boundary inverse-proportionally to fine-scale conductivities in elements adjacent to the edge; that is, $\Delta\varphi_i = \Delta\varphi \cdot (1/k_i) \cdot d_i / (\sum_i \cdot (1/k_i) \cdot d_i)$.

For simplicity reasons in our computations we assigned a constant head equal zero on the western boundary of the block, and a constant head equal 4 on the eastern edge. As for the flux boundary conditions we assumed a uniform inflow flux from the western boundary and an equal uniform outflow flux through the eastern edge, with no-flow boundary conditions on the horizontal edges. The two sets of boundary conditions were consistent for a block with homogeneous conductivity equal to 10, which is in agreement with setting the mean-log conductivity equal to 1 while generating the test fields.

3.2 Double Constraint Method – computational results

Computations follow the steps described in Section 2.1. Solutions obtained for the two sets of boundary conditions for initial conductivity distributions are plotted in Fig. 3. Conductivities were updated following (4), thus isotropy of conductivities was ensured.

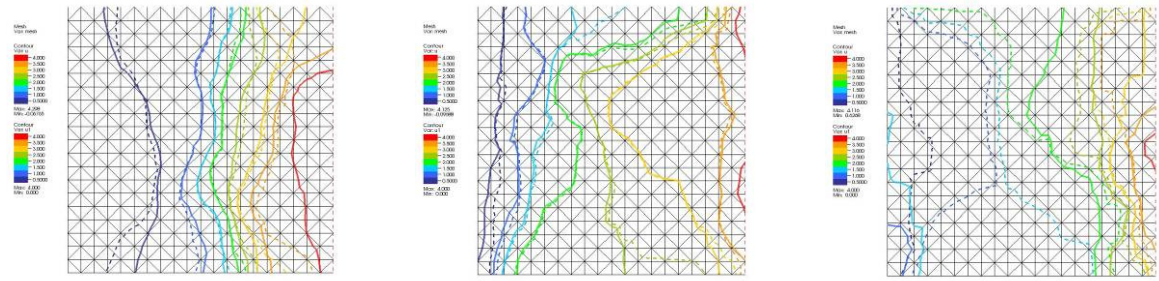

Case 1 Case 2 Case 3

Figure 3: Isolines of heads computed for initial conductivities. Solid lines – solution with the flux boundary conditions. Dashed lines – solution of the Dirichlet problem.

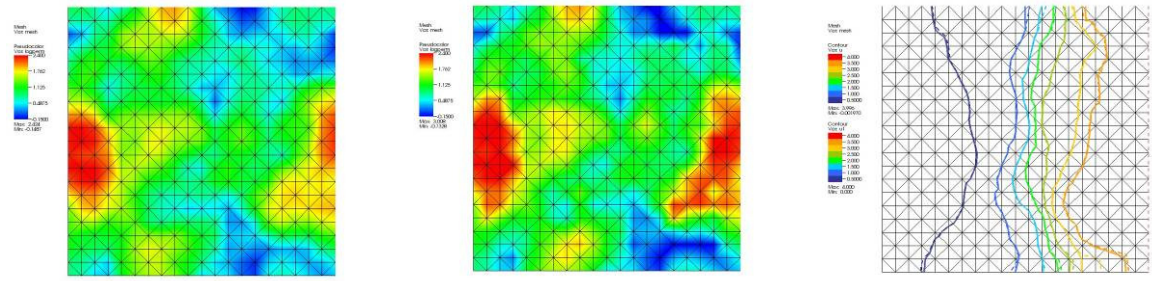

a) b) c)

Figure 4: Case 1. a) Conductivities after 1st iteration, b) after 12th iteration, c) solutions after 12th iteration.

Along with the modified conductivities we present the solutions obtained for two sets of boundary conditions. Fig. 4 gives results obtained for the *Case_1*. A good agreement is

obtained already after a very few iterations. As could be expected, in *Case_2* and *Case_3* more iterations are needed; see Figs. 5 and 6.
Because of the way the boundary conditions are defined at the fine scale, it was necessary to keep the conductivity values in elements adjacent to the boundary constant – otherwise the procedure may fail due to the strong relationship between the boundary conditions and the conductivities in the boundary elements. While computing new conductivities, following (4) or (5), care must be taken to avoid division by zero by special exception handling, for instance keeping conductivities in a given element unchanged. In order to avoid too high conductivities it is recommended to impose an upper limit.

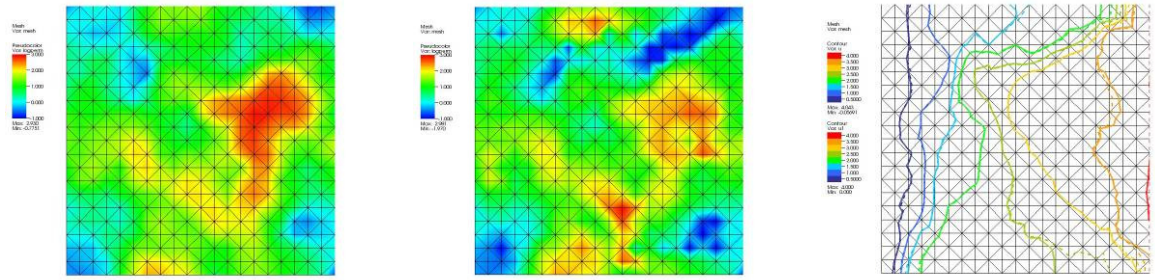

a) b) c)

Figure 5: Case 2. a) Conductivities after 1st iteration, b) after 12th iteration, c) solutions after 12th iteration.

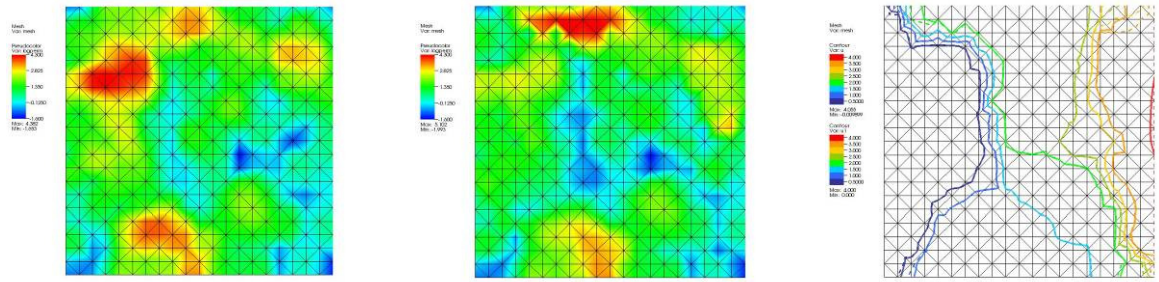

a) b) c)

Figure 6: Case 3. a) Conductivities after 1st iteration, b) after 12th iteration, c) solutions after 12th iteration.

	Case 1	Case 2	Case 3
after 1st iteration	1,026911	2,132962	2,030169
after 4th iteration	0,968439	1,204608	1,753328
after 12th iteration	0,996565	1,031892	1,098204

Table 2: Anisotropy ratio during iterations

It is interesting to study the anisotropy ratios α which were recorded during the iterations. In Table 2 we give values of anisotropy ratios averaged over mesh elements. As expected, the level of initial heterogeneity influences the convergence of the DC method.

4 CONCLUSIONS

We defined a downscaling problem and presented the Double Constraint method, an efficient direct inversion method. The DC method is very robust and produces satisfactory solutions even in case of initial patterns with high contrasts in conductivities. It is relatively easy in implementation; if a general purpose flow solver is used then it is enough to extend it with an external loop of iterations. Moreover, it allows adding *ad hoc* modifications as well as the introduction of additional restrictions, for instance keeping conductivities in given elements unchanged, or imposing upper or lower limits to conductivity values.

To increase the flexibility of the DC method it is considered to combine it as a "postprocessor" with the Constrained Back Projection method[9].

Acknowledgements

The author would like to thank Wouter Zijl from Dept. of Hydrology and Hydraulic Engineering, Vrije Universiteit Brussel, for many discussions and valuable comments.

REFERENCES

[1] G.K. Brouwer, P.A. Fokker, F. Wilschut, W. Zijl, "A direct inverse model to determine permeability fields from pressure and flow rate measurements", *Math. Geosci.,* **40**, 907-920 (2008).

[2] J.E. Chambers, O. Kuras, P.I. Meldrum, R.D. Ogilvy, and J. Hollands, "Electrical resistivity tomography applied to geologic, hydrogeologic, and engineering investigations at a former waste-disposal site", *Geophysics*, **71**, B.231-B239 (2006).

[3] A. Farcas, L. Elliott, D.B. Ingham, D. Lesnic, "An inverse dual reciprocity method for hydraulic conductivity identification in steady groundwater flow", *Advances in Water Resources*, **27**, 223-235 (2004).

[4] S. Fomel, "Shaping regularization in geophysical-estimation problems", *Geophysics*, **72**, R29-R36 (2007).

[5] L. Borcea, V. Druskin, F.G. Vasquez, "Electrical impedance tomography with resistor networks", *Inverse Problems*, **24**, 035013 (2008).

[6] V. Kolehmainen, J.P. Kaipio, H.R.B. Orlande, "Reconstruction of thermal conductivity and heat capacity using a tomographic approach", *Int. Journal of Heat and Mass Transfer*, **51**, 1866-1876 (2008).

[7] A. Wexler, "Electrical impedance imaging in two and three dimensions", *Clin. Phys. Physiol. Meas*., **9**, Suppl. A, 29-33 (1988).

[8] A. Trykozko, G. Brouwer, W. Zijl, "Downscaling – a complement to homogenization", *Int. Journ. Of. Num. Analysis and Modeling*, **5**, Supp, 157-170 (2008).

[9] G.A. Mohammed, W. Zijl, O. Batelaan, and F. De Smedt, "Comparison of two mathematical models for 3D groundwater flow: block-centered heads and edge-based stream functions", *Transport in Porous Media*, **79**, 469-485 (2009).

[10] J. Gottlieb, P. Dietrich, "Identification of the permeability distribution in soil by hydraulic tomography", *Inverse Problems*, **11**, 353-360 (1995).

[11] Olaf Cirpka, http://matlabdb.mathematik.uni-stuttgart.de/download.jsp?MP_ID=31.